

Transfer Hydrogenation of Alkenes Using Ethanol Catalyzed by A NCP Pincer Iridium Complex: Scope and Mechanism

Yulei Wang, Zhidao Huang, Xuebing Leng, Huping Zhu, Guixia Liu, and Zheng Huang

J. Am. Chem. Soc., **Just Accepted Manuscript** • Publication Date (Web): 08 Mar 2018

Downloaded from <http://pubs.acs.org> on March 8, 2018

Just Accepted

"Just Accepted" manuscripts have been peer-reviewed and accepted for publication. They are posted online prior to technical editing, formatting for publication and author proofing. The American Chemical Society provides "Just Accepted" as a service to the research community to expedite the dissemination of scientific material as soon as possible after acceptance. "Just Accepted" manuscripts appear in full in PDF format accompanied by an HTML abstract. "Just Accepted" manuscripts have been fully peer reviewed, but should not be considered the official version of record. They are citable by the Digital Object Identifier (DOI®). "Just Accepted" is an optional service offered to authors. Therefore, the "Just Accepted" Web site may not include all articles that will be published in the journal. After a manuscript is technically edited and formatted, it will be removed from the "Just Accepted" Web site and published as an ASAP article. Note that technical editing may introduce minor changes to the manuscript text and/or graphics which could affect content, and all legal disclaimers and ethical guidelines that apply to the journal pertain. ACS cannot be held responsible for errors or consequences arising from the use of information contained in these "Just Accepted" manuscripts.



Transfer Hydrogenation of Alkenes Using Ethanol Catalyzed by A NCP Pincer Iridium Complex: Scope and Mechanism

Yulei Wang, Zhidao Huang, Xuebing Leng, Huping Zhu, Guixia Liu, and Zheng Huang*

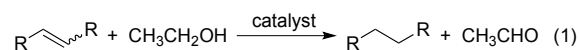
State Key Laboratory of Organometallic Chemistry, Center for Excellence in Molecular Synthesis, Shanghai Institute of Organic Chemistry, University of Chinese Academy of Sciences, Chinese Academy of Sciences, 345 Lingling Road, Shanghai 200032, China.

ABSTRACT: The first general catalytic approach to effecting transfer hydrogenation (TH) of unactivated alkenes using ethanol as the hydrogen source is described. A new NCP-type pincer iridium complex ($^{BQ}\text{-NC}^{\text{O}}\text{P}$)IrHCl containing a rigid benzoquinoline backbone has been developed for efficient, mild TH of unactivated C–C multiple bonds with ethanol, forming ethyl acetate as the sole byproduct. A wide variety of alkenes, including multisubstituted alkyl alkenes, aryl alkenes, and heteroatom-substituted alkenes, as well as *O*- or *N*-containing heteroarenes and internal alkynes, are suitable substrates. Importantly, the ($^{BQ}\text{-NC}^{\text{O}}\text{P}$)Ir/EtOH system exhibits high chemoselectivity for alkene hydrogenation in the presence of reactive functional groups, such as ketones and carboxylic acids. Furthermore, the reaction with $\text{C}_2\text{D}_5\text{OD}$ provides a convenient route to deuterium-labeled compounds. Detailed kinetic and mechanistic studies have revealed that monosubstituted alkenes (e.g., 1-octene, styrene) and multisubstituted alkenes (e.g., cyclooctene (COE)) exhibit fundamental mechanistic difference. The OH group of ethanol displays a normal kinetic isotope effect (KIE) in the reaction of styrene, but a substantial *inverse* KIE in the case of COE. The catalysis of styrene or 1-octene with relatively strong binding affinity to the Ir(I) center has ($^{BQ}\text{-NC}^{\text{O}}\text{P}$)Ir^I(alkene) adduct as an off-cycle catalyst resting state, and the rate law shows a positive order in EtOH, inverse first-order in styrene, and first-order in the catalyst. In contrast, the catalysis of COE has an off-cycle catalyst resting state of ($^{BQ}\text{-NC}^{\text{O}}\text{P}$)Ir^{III}(H)[O(Et)⋯HO(Et)⋯HOEt] that features a six-membered iridacycle consisting of two hydrogen-bonds between one EtO ligand and two EtOH molecules, one of which is coordinated to the Ir(III) center. The rate law shows a negative order in EtOH, zeroth-order in COE, and first-order in the catalyst. The observed *inverse* KIE corresponds to an *inverse* equilibrium isotope effect for the pre-equilibrium formation of ($^{BQ}\text{-NC}^{\text{O}}\text{P}$)Ir^{III}(H)(OEt) from the catalyst resting state via ethanol dissociation. Regardless of the substrate, ethanol dehydrogenation is the slow segment of the catalytic cycle, while alkene hydrogenation occurs readily following the rate-determining step, that is, β -hydride elimination of ($^{BQ}\text{-NC}^{\text{O}}\text{P}$)Ir(H)(OEt) to form ($^{BQ}\text{-NC}^{\text{O}}\text{P}$)Ir(H)₂ and acetaldehyde. The latter is effectively converted to innocent ethyl acetate under the catalytic conditions, thus avoiding the catalyst poisoning via iridium-mediated decarbonylation of acetaldehyde.

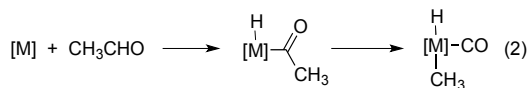
1. INTRODUCTION

The catalytic hydrogenation is a reaction with enormous applicability, ranging from fine chemical to pharmaceutical and agrochemical synthesis.¹ Transfer hydrogenation (TH), as an alternative to direct hydrogenation using molecular H₂, has garnered tremendous attention because the process does not require the use of flammable gas nor elaborate experimental equipments.² In addition, the catalytic TH reactions have the potential applications in energy storage³ and biotechnologies.⁴ While catalytic methods for TH of ketones, imines, and polarized alkenes (e.g., α , β -unsaturated ketones) have been well-established,^{5–8} these catalytic systems often exhibit low efficiency and narrow scope for TH reactions of non-polarized, unactivated C–C double bonds. Among various hydrogen donors, amine–borane adducts,⁹ water–B₂(OH)₄/B₂pin₂ combination,¹⁰ formic acid,¹¹ and isopropanol^{12,13} have proven effective for transition metal-catalyzed hydrogenation of non-polarized unsaturated C–C bonds.

Ethanol is a highly attractive hydrogen source given its abundance, sustainability, and environmentally benign nature. Although a number of transition metal complexes are known to catalyze TH with *i*PrOH,^{12,13} ethanol has been seldom applied to catalytic TH.^{14–16} Very recently, Grützmacher reported Rh complex-catalyzed TH of ketones¹⁴ and Swamy disclosed Pd complex-catalyzed TH of ynamides¹⁵ with ethanol. Unfortunately, both systems are inactive for TH of unactivated C–C double bonds.^{14,15} Indeed, homogeneously catalytic TH reactions of unactivated alkenes using EtOH (eq 1) have remained unknown.



The limited success of EtOH relative to *i*PrOH in transition metal-catalyzed TH reactions can be attributed to the catalyst deactivation caused by the alcohol dehydrogenation product: in contrast to acetone, acetaldehyde readily undergoes metal-mediated decarbonylation, leading to catalytically inactive metal carbonyl species (eq 2).¹⁷



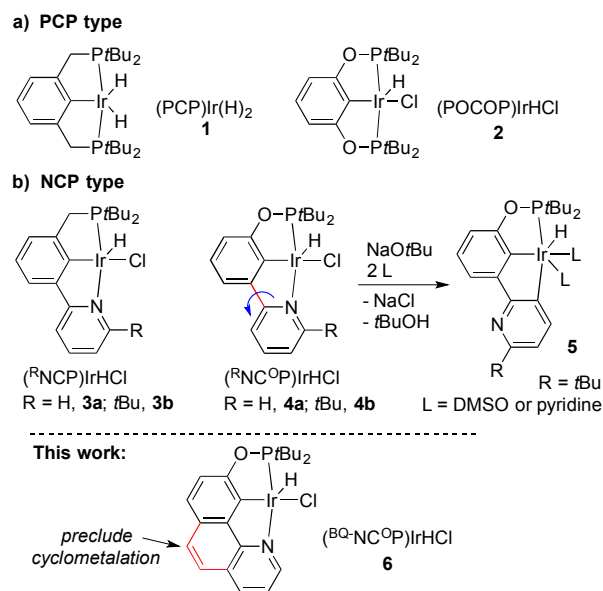
Featuring high thermostability, PCP-type pincer iridium complexes (e.g., (PCP)Ir(H)₂ **1**¹⁸ and (POCOP)IrHCl **2**,¹⁹ Chart 1a) are powerful class of catalysts for organic substrate desaturation, mostly for alkane dehydrogenation.²⁰ Inspired by the precedents, our group has been interested in the development of pyridine-containing NCP-type pincer iridium complexes (Chart 1b), with a focus on understanding the effects caused by the phosphine-to-pyridine substitution on the electronic properties and catalytic performance.²¹ Among a series of NCP complexes, (NC^{OP})IrHCl **4a** has been found to be moderately active for transfer dehydrogenation of alkanes with *tert*-butylethylene as the hydrogen acceptor,^{21a} and highly efficient for α -alkylation of esters^{21c} and amides^{21d} with primary alcohols as the alkylating reagents. The juxtaposition of these results suggests that the NCP-type iridium catalyst should be effective for the TH of alkene with alcohol. The main challenge now lies in the use of ethanol as the hydrogen source for the hydrogenation of unactivated alkenes. Here, we report that a new NCP pincer iridium complex containing a rigid benzoquinoline backbone (^{BQ}NC^{OP})IrHCl (**6**, Chart 1b) is a versatile and selective catalyst for the TH of unactivated C–C multiple bonds with ethanol under mild conditions. During the TH transformation, ethanol is effectively converted to ethyl acetate,²² instead of acetaldehyde, which helps avoid the catalyst poisoning via decarbonylation. The system enables the hydrogenation of not only unactivated alkenes with varying electronic and steric properties, but *O* and *N*-containing heteroarenes and internal alkynes as well. Kinetic and mechanistic studies provide insight into the rate-determining step and the catalyst resting states for different classes of alkenes, and elucidate the origin of the unique compatibility between the (^{BQ}NC^{OP})Ir catalyst and EtOH.

2. RESULTS AND DISCUSSION

2.1. Synthesis of (^{BQ}NC^{OP})IrHCl **6.** Our earlier studies on (^{*t*Bu}NC^{OP})IrHCl **4b** revealed that, upon on dehydrochlorination, the pyridine moiety can dissociate from the metal center. The subsequent rotation of the pyridine ring and cyclometalation via C(sp²)–H bond oxidative addition leads to an Ir(III) hydride species, which can be trapped by two coordinating molecules, such as DMSO and pyridine, to form a six-coordinate complex **5** (see Chart 1b).²³ We hypothesized that the generation of such an Ir(III) species might have a detrimental effect on catalysis involving substrate activation by an Ir(I) species. To circumvent the cyclometalation event, in this work we designed a new NCP ligand containing a rigid benzoquinoline skeleton (^{BQ}NC^{OP}) (Chart 1b).

The building block for the ligand precursor, 9-MeO-benzoquinoline **7**, was synthesized according to the literature procedure.²⁴ Deprotection of the MeO group with HBr, followed by deprotonation with NaH, and treatment with *t*Bu₂PdCl, generated ^{BQ}NC(H)^{OP} **9** in 73% yield. Metalation of **9** with [Ir(COD)Cl]₂ under H₂ atmosphere in

Chart 1. PCP and NCP pincer-ligated iridium complexes



refluxing toluene produced (^{BQ}NC^{OP})IrHCl **6** in 88% yield (Figure 1).

Complex **6** has been characterized by NMR spectroscopy and elemental analysis. The Ir–H resonance appears at δ 40.56 ppm in CDCl₃, which is consistent to that observed for the pincer-ligated Ir(III) hydrido chloride complexes adopting a square pyramidal geometry,^{21a,21b} in which the hydride is *trans* to a vacant coordination site. Growing single crystals of **6** in THF resulted in the formation of a six-coordinate THF-bound complex, (^{BQ}NC^{OP})IrHCl(THF) (**6**-THF), as determined by X-ray diffraction analysis (Figure 1).

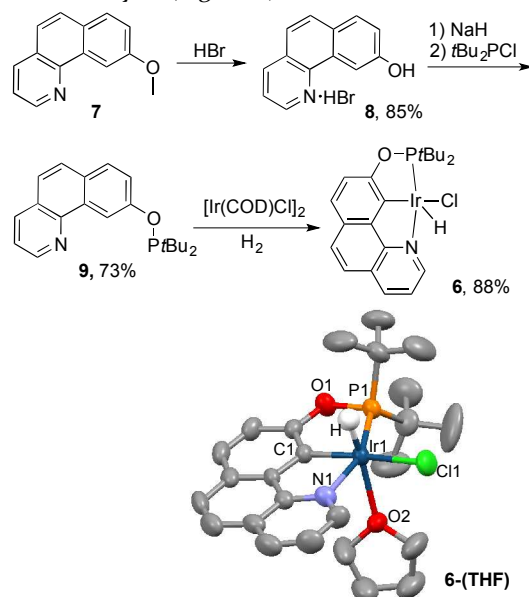


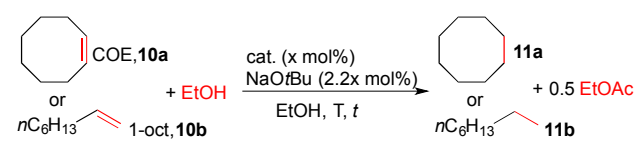
Figure 1. Synthetic route to (^{BQ}NC^{OP})IrHCl **6** and ORTEP diagram of **6**-(THF).

2.2. Catalyst Evaluation for TH of Alkenes with EtOH. The series of NCP pincer Ir(III) complexes, togeth-

er with the classical PCP complexes, were tested for the catalytic TH of unactivated alkenes with EtOH. Cyclooctene (COE, **10a**) and 1-octene (1-oct, **10b**) were chosen as the model substrates because they represent unactivated internal and terminal alkenes, respectively. The results are summarized in Table 1. Upon activation with NaOtBu, (NCP)IrHCl (**3a**) (1 mol%) gave only 9% cyclooctane (COA, **11a**) after 12 h at 30 °C for the reaction of COE in EtOH (entry 1). Its variant (NC^{OP})IrHCl (**4a**) with a O-atom linker between the P donor and the backbone in the ligand showed improved activity, furnishing 68% COA (entry 3). Complexes **3b** and **4b** bearing a *t*Bu substituent at the C₆ position of the pyridine ring are inactive for the TH (entries 2 and 4). The PCP pincer complexes (entries 5 and 6), as well as other common late transition metal complexes, such as Rh(PPh₃)₃Cl and Ru(PPh₃)₃(CO)HCl, effect little, if any, catalysis (see Supporting Information).

Encouragingly, the new complex (B^Q-NC^{OP})IrHCl (**6**), upon activation with NaOtBu, is highly productive for the TH of COE with EtOH, furnishing COA in quantitative yield after 12 h at 30 °C (entry 7). EtOAc was the only detectable byproduct, indicating that acetaldehyde resulting from EtOH dehydrogenation reacts rapidly with another molecule of EtOH to yield hemiacetal, which is dehydrogenated further to EtOAc, probably under the influence of iridium catalysis.²² At elevated temperature (60 °C), the process with 0.25 mol% of **6** for 2 h or with 0.1 mol% of **6**

Table 1. Pincer Iridium Catalysts for TH of COE and 1-Oct with EtOH^a



Entry	Alkene	cat.	x mol%	T (°C)	t (h)	yield (%)
1	COE	3a	1	30	12	9
2	COE	3b	1	30	12	<1
3	COE	4a	1	30	12	68
4	COE	4b	1	30	12	<1
5	COE	(PCP)IrHCl	1	30	12	<2
6	COE	2	1	30	12	10
7	COE	6	1	30	12	>99
8	COE	6	1	60	0.33	>99
9	COE	6	0.25	60	2	>99
10 ^b	COE	6	0.1	60	3	>99
11 ^c	COE	6	0.25	60	1	>99
12	1-oct	3a	1	30	12	>99
13	1-oct	3b	1	30	12	<15
14	1-oct	4a	1	30	12	>99
15	1-oct	4b	1	30	12	<45
16	1-oct	(PCP)IrHCl	1	30	12	2
17	1-oct	2	1	30	12	2
18	1-oct	6	1	30	12	>99
19	1-oct	6	1	60	0.33	>99

^aConditions: **10a** or **10b** (0.5 mmol), cat. (5 μmol), NaOtBu (11 μmol), solvent (1 mL). Yield was determined by GC using mesitylene as an internal standard. ^b**10a** (2 mmol), EtOH (2 mL). ^c**10a** (2 mmol), EtOH (6 mmol).

for 3 h reached a full conversion (entries 9, 10). Performing the TH with three equiv of EtOH relative to COE afforded the desired product in >99% yield in 1h, indicating a large excess of EtOH is not required for a high conversion (entry 11). While *i*PrOH proved to be a suitable hydrogen donor, the run with MeOH gave only 13% COA (see Supporting Information).

Examination of these NCP and PCP pincer iridium catalysts for the TH of 1-oct with EtOH revealed that (NCP)IrHCl (**3a**, entry 12), (NC^{OP})IrHCl (**4a**, entry 14), and (B^Q-NC^{OP})IrHCl (**6**, entry 18), are effective catalysts, but the *t*Bu-substituted complexes, (*t*BuNCP)IrHCl (**3b**, entry 13) and (*t*BuNC^{OP})IrHCl (**4b**, entry 15), showed low level of activity. The PCP complexes are inactive for the TH (entries 16 and 17). Finally, the TH reaction with **6** at 60 °C was found to be complete in 20 min (entry 19).

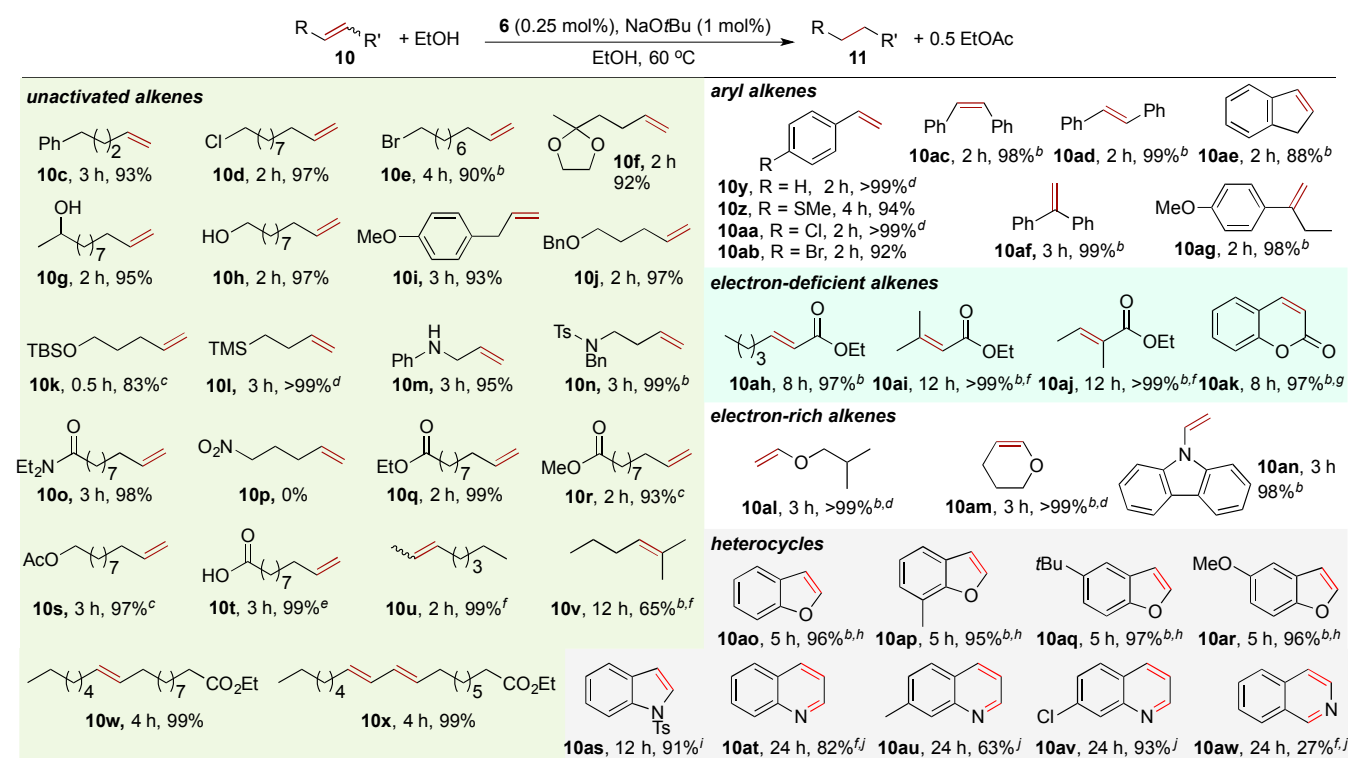
The results shown in Table 1 illustrate the profound influence of the pincer ligands on the catalytic activity. Given its superior performance in the TH reactions of both internal and terminal alkenes, we focused on **6**/NaOtBu to explore the scope of various types of C–C multiple bonds using EtOH as the hydrogen donor.

2.3. Reaction Scope. The (B^Q-NC^{OP})Ir/EtOH combination ("Free" (B^Q-NC^{OP})Ir is proposed to be generated in situ upon activation of **6** with NaOtBu¹⁹) can effect the reductions of a wide range of unactivated C–C multiple bonds with varying electronic and steric properties (Table 2). Most reactions employed low catalyst loadings (0.25 mol% **6**), and occurred at 60 °C within hours, giving the desired products in high isolated yields (>90%).

2.3.1. Alkyl Alkenes. Simple α-olefins, such as 1-oct (**10b**), 5-Ph-1-pentene (**10c**), were reduced smoothly. A variety of functional groups, including Cl (**10d**), Br (**10e**), ketal (**10f**), and even unprotected OH group (**10g**, **10h**), were unaffected under the catalytic conditions. Allyl benzene derivatives (**10i**) are suitable substrates. Benzyl ether (**10j**) and silyl ether (**10l**) that are subject to C–O or Si–O cleavage under H₂/Pd/C catalysis, underwent selective C–C double bond reduction with the protecting group remaining intact under our catalytic conditions. Nitrogen-containing functionalities, such as amide, and secondary and tertiary amines, are compatible with the catalyst (**10m–o**). However, attempts to reduce a nitro-functionalized alkene were unsuccessful (**10p**).

The TH reactions of ester-containing unactivated alkenes demonstrate the high chemoselectivity of (B^Q-NC^{OP})Ir/EtOH for the C–C double bond reduction (**10q–s**). Methyl undec-10-enoate (**10r**) and undec-10-en-1-yl acetate (**10s**) gave high yields of the desired products without detectable ester exchange under pH-neutral conditions.²⁵ Remarkably, 1-alkene containing a terminal carboxylic acid functionality (**10p**) was selectively reduced in the presence of one equiv of NaOtBu.

In addition to cycloalkane (COE), the catalytic system is also effective for the hydrogenation of multisubstituted, acyclic internal alkenes (**10u–x**). Notably the reactions of oleate (**10w**) and linoleate (**10x**) afforded the saturated products in quantitative yields. Two conjugated double

Table 2. Scope of Ir-Catalyzed TH of C–C Double Bonds with EtOH^a

^aConditions: **10** (0.5 mmol), **6** (0.25 mol%), NaOtBu (1 mol%) in EtOH (1 mL) at 60 °C. Yields shown are of isolated products. ^b**6** (1 mol%), NaOtBu (2.2 mol%). ^c**6** (1 mol%), NaOtBu (1 mol%). ^dYield was determined by ¹H NMR analysis of the crude reaction mixtures using mesitylene as an internal standard. ^eEtOH (2 mL), NaOtBu (1.05 equiv). ^fYield was determined by GC. ^gReduced alcoholysis product was obtained. ^hEtOH (0.5 mL). ⁱ**6** (2 mol%). ^j**6** (5 mol%), at 80 °C.

bonds in **10x** were both hydrogenated with high efficiency.

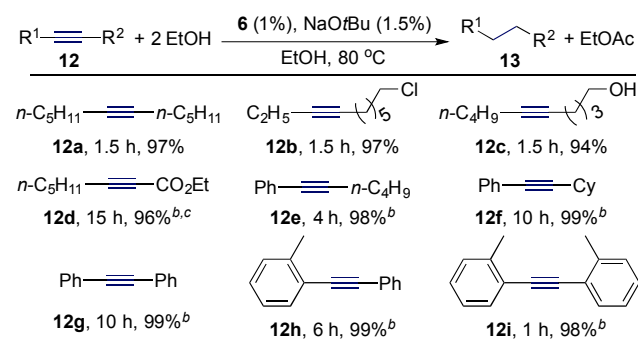
Styrene and its derivatives (**10y–ag**) are also reactive towards the TH. Substrates containing a thioether (**10z**) or halide (**10aa**, **10ab**) substituent in the *para*-position were reduced cleanly to the desired products. High conversions were obtained from the TH reactions of *cis*- (**10ac**) and *trans*-stilbene (**10ad**), as well as indene (**10ae**). The reductions of diaryl and arylalkyl 1,1-disubstituted alkenes (**10af**, **10ag**) occurred in excellent yields.

The polarized C–C double bonds of α,β -unsaturated esters (**10ah–aj**) underwent selective hydrogenation, as well. The trisubstituted double bonds of **10ai** and **10aj** were reduced in quantitative yield. The hydrogenation of the double bond of coumarin (**10ak**) was accompanied by ring-opening via ester exchange, resulting in the formation of ethyl melilotate.

Catalytic methods for the TH of vinyl ethers or vinyl amines with alcohol have remained unknown, probably due to the relatively high insertion barriers for electron-rich alkenes into metal-hydride.²⁶ A brief exploration of electron-rich alkenes revealed that (^{BQ}-NC^{OP})Ir/EtOH is capable of reducing *O*- or *N*-attached alkenes with high efficiency. For example, the *i*BuO-substituted alkene (**10al**) and cyclic vinyl ether (**10am**), were hydrogenated in >99% yield. *N*-ethylcarbazole was obtained in 98% isolated yield via the TH of *N*-vinylcarbazole (**10an**).

2.3.2. Heteroarenes. Reduction of heteroarenes is thermodynamically unfavorable. Prior to this work, there has been only one example of TH of benzofuran with alcohol, but with low selectivity: a Raney Ni-catalyzed TH of benzofuran with *i*PrOH gave considerable amounts of ring-opening side-products due to the C–O cleavage.²⁷ Remarkably, (^{BQ}-NC^{OP})Ir/EtOH enabled the selective reduction of benzofuran and its derivatives (**10ao–ar**), giving dihydrobenzofurans in $\geq 95\%$ isolated yields (Table 3). *N*-tosyl-indole (**10as**) was also suitable to the TH. The C=C and C=N bonds of quinoline and its derivatives (**10at–av**) were reduced in useful yields. Isoquinoline (**10aw**), however, exhibited low reactivity.

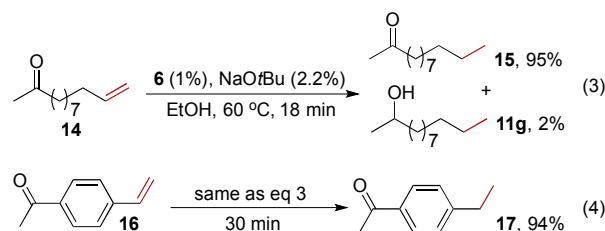
2.3.3. Alkynes. The (^{BQ}-NC^{OP})Ir/EtOH system was further applied to full reduction of internal alkynes (Table 3). Unactivated aliphatic internal alkynes, 6-dodecyne and alkynes bearing Cl or OH functionality (**12a–c**), were efficiently reduced using 1 mol% of catalyst at 80 °C. The electron-deficient internal alkyne, ethyl 2-octynoate (**12d**), and diaryl-substituted internal alkynes (**9e–i**), gave the reduction products in >95% isolated yields using 2 mol% of **6**. A comparison of the reactivity of diaryl alkynes (**12g–i**) revealed that the more sterically hindered substrate is more reactive than the less hindered one, as judged by the reaction times required for high conversions.

Table 3. Scope of Ir-Catalyzed TH of Alkynes with EtOH^a

^aConditions: **12** (0.5 mmol), **6** (1 mol%), NaOtBu (1.5 mol%), EtOH (2.0 mL) at 80 °C. Yields shown are of isolated products. ^b**6** (2 mol%), NaOtBu (3 mol%). ^cAt 100 °C.

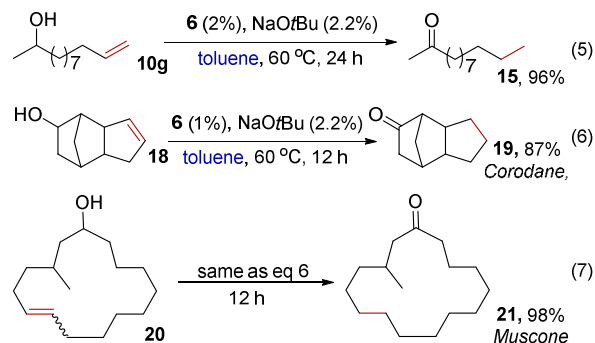
2.4. Chemoselective (^{BQ}NC^OP)Ir-Catalyzed TH of Non-conjugated Ketone-Functionalized Alkenes. The wide functional-group tolerance of our (^{BQ}NC^OP)Ir/EtOH system demonstrated by the examples of functionalized alkenes promoted us to explore more challenging substrates, non-conjugated ketone-functionalized alkenes. In general, the polar C=O bonds are more reactive than the non-polarized alkenes toward transition metal-catalyzed TH, rendering the selective reduction of the latter in the presence of the isolated ketone unit difficult. In fact, the known examples of selective C=C hydrogenations are limited to α , β -unsaturated ketones.⁷ The substrates containing non-conjugated C=C and C=O bonds undergo either selective C=O hydrogenation²⁸ or reduction of both.^{12b,28}

To access the ability of (^{BQ}NC^OP)Ir/EtOH for chemoselective reduction of C=C over C=O bond, 11-dodecen-2-one (**14**) was submitted to the standard catalytic conditions. ¹H NMR analysis showed the reaction formed 95% dodecan-2-one (**15**) and 2% over-reduction product (**11g**) after 18 min (eq 3). One possible route to **15** is the initial hydrogenation of the C=O bond of **14** to form 11-dodecen-2-ol (**10g**), followed by double bond chain-running isomerization.²⁹ However, the facile TH of **10g** to form **11g** under the catalytic conditions as shown in Table 2 suggests that such a pathway is unlikely. In addition, the exclusive reduction of the C=C bond in the reaction of 4-acetylstyrene (**16**, 94%), with no evidence for the C=O hydrogenation (eq 4), clearly demonstrates the desired chemoselectivity (chain-running isomerization cannot occur in this case).

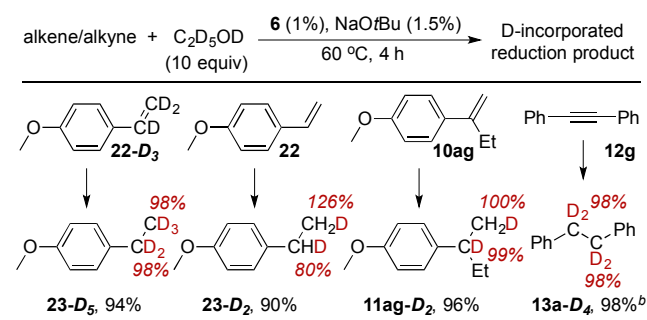


2.5. Disproportionation Reaction. The Ir-catalyzed TH reaction can occur in a formal intramolecular manner, as exemplified by the conversion of 11-dodecen-2-ol (**10g**) to dodecan-2-one (**15**, 96%) in toluene *without an external*

hydrogen donor (eq 5). The intramolecular TH allowed a one-step synthesis of corodane from its alcohol precursor **18** (eq 6). Such a conversion involving a tricyclodecane structure, again, indicates that the double bond chain-running isomerization is not a viable pathway. The utility of Ir-catalyzed TH was further demonstrated by the high-yielding synthesis of muscone **21**, a primary contributor to the odor of musk (eq 7). By comparison, the published routes to corodane³⁰ and muscone³¹ from their alcohol precursors require two steps because the alcohol oxidation and the internal olefin reduction operate under different conditions.



2.6. Deuterium-Incorporation by TH with C₂D₅OD. Using easily accessible ethanol-*D*₆ as the deuterium donor enables facile deuterium-incorporation into the reduction products (Table 4). For example, treatment of a styrene derivative **22-D₃** bearing three D-atoms in the olefinic positions with 10 equiv C₂D₅OD gave **23-D₅** with a perdeuterated Et group. The reaction of **22**, however, resulted in an uneven D-distribution: the D-incorporation level in the benzylic position (80%) was lower than that in the Me group (126%), implying reversible 2,1-insertion of alkene into the Ir-D bond. By contrast, the D-atom was added equally to the C-C double bond of 1,1-disubstituted alkene **10ag**, which can be attributed to the preferential 1,2-insertion over 2,1-insertion, presumably due to the steric influence. Moreover, D-atom was present only at the tertiary carbon and in the attached Me group (**11ag-D₂**), thus ruling out the possibility of olefin isomerization prior to the reduction, at least for this substrate. Finally, the run of diphenylacetylene with C₂D₅OD yielded the product with a perdeuterated ethylene linker between two Ph

Table 4. Deuterium-Atom Incorporation Using C₂D₅OD^a

^aConditions: substrate (0.5 mmol), **6** (1 mol%), NaOtBu (1.5 mol%), EtOH (2.0 mL). Yields shown are of isolated products. ^b**6** (5 mol%), NaOtBu (11 mol%), at 80 °C, 48 h.

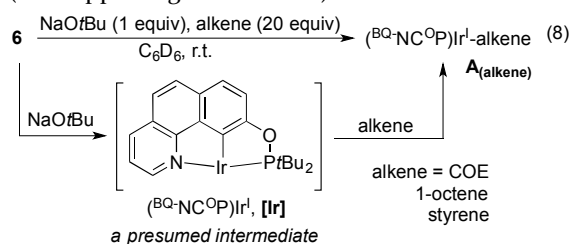
groups (**13a-D₄**). Although effective, it is worth noting that the *selective* D-incorporation by this method is limited to substrates that are reluctant to isomerization.

2.7. Exploring the Mechanism of Ir-Catalyzed TH of Alkene with EtOH.

2.7.1. Studies on the Catalyst Resting State(s).

Monitoring the catalytic reactions of different classes of alkenes, COE, 1-oct, and styrene by NMR spectroscopy provided insight into the resting state(s) of the catalyst.

Treatment of **6** with 1.5 equiv of NaOtBu and 20 equiv of COE, 1-oct, or styrene in C₆D₆ formed the corresponding alkene complex (^{BQ}-NC^OP)Ir^I(alkene), **A**_(alkene) (alkene = COE, 1-oct, or styrene), presumably via the 14e⁻ Ir(I) intermediate, (^{BQ}-NC^OP)Ir^I, [**Ir**] (eq 8). **A**_(sty) (sty = styrene) is isolable, but attempts to isolate **A**_(COE) and **A**_(1-oct) by evaporating volatiles failed and furnished unidentified species. Nevertheless, complexes **A**_(COE) and **A**_(1-oct) are stable in solution in the presence of the corresponding alkene, and characterized by ¹H and ³¹P NMR spectroscopies (see Supporting Information).



To mimic the catalytic conditions, EtOH (170 equiv relative to Ir) was then added to the C₆D₆ solution of **A**_(alkene) and free alkene (~19 equiv). Monitoring the catalytic TH reaction of 1-oct with EtOH by ³¹P NMR showed that **A**_(1-oct) was the only detectable Ir species over the course of 3 h. After 4 h with 90% conversion of 1-oct, **A**_(1-oct) was still the major species (83%), with a new iridium species **B** present in small concentration (17%). **B** did become the major species after 5 h when 1-oct was fully converted to *n*-octane (97%) and internal octenes (~3%, the isomerization products). Likewise, ³¹P and ¹H NMR experiments revealed that **A**_(sty) was the dominant species, even when the catalytic TH reaction of styrene with EtOH was nearly complete (see NMR data in Supporting Information).

In contrast to the reactions of 1-oct and styrene, the main catalyst resting state for the TH reaction of COE is **B**, even at the beginning of the reaction with high [COE]. The ³¹P signal for **A**_(COE) at δ 168.0 ppm disappeared, and a single species at δ 158.6 ppm matching the chemical shift of **B** appeared immediately upon the addition of EtOH. Complex **B** has remained as the major resting state until the very late stages of the reaction (95% conversion of COE). Multiple species were detected by ³¹P NMR after the full consumption of COE.

Significant effort has then been focused on the determination of the structure of **B**. This complex is detectable only in the presence of excess EtOH.³³ A characteristic ³¹P-coupled Ir–H doublet, was detected at δ -29.79 ppm by ¹H NMR spectroscopy (*J*_{P-H} = 24.9 Hz at 20 °C). The ³¹P NMR spectrum exhibits a line-broadening resonance (*w*_{1/2} = 17.8

Hz at 20 °C), implying a fluxional behavior on the NMR time scale. Cooling the NMR sample to -75 °C resulted in no significant change of the ³¹P signal (δ 158.7 ppm, *w*_{1/2} = 21.8 Hz at -75 °C), but two new multiplets at δ 4.28 and 4.12 ppm were observed by the low-temperature ¹H NMR (These two signals could not be observed at 20 °C). ¹H–¹³C and ¹H–¹H COSY NMR experiments at -75 °C unambiguously established that these two multiplets are due to two diastereotopic protons of the OCH₂CH₃ ligand (Figure 2a). These NMR data indicate that **B** contains Ir–H and Ir–OEt moieties. It is pertinent to note that the Ir–H signal for **B** (-29.79 ppm at 20 °C) is significantly downfield-shifted as compared to those for the five-coordinate Ir(III) complex **6** (-40.56 ppm) and other five-coordinate pincer Ir(III) hydride complexes reported in literature,^{21a,21b} implying that the coordination site *trans* the hydride in **B** is occupied.

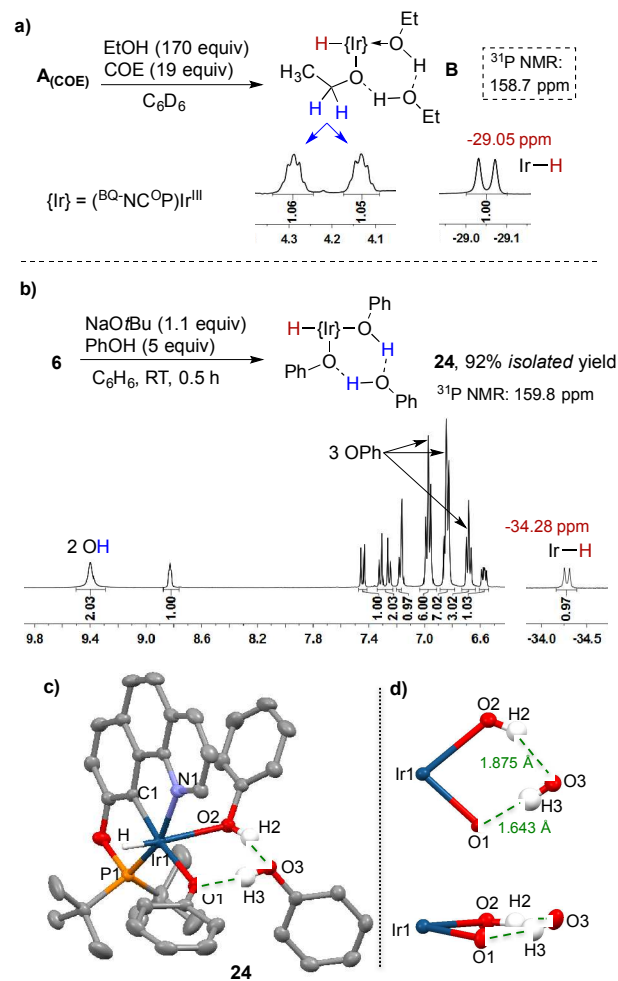
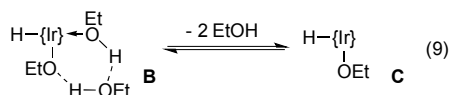


Figure 2. a) Formation of complex **B** and its partial ¹H NMR spectra at -75 °C. b) Synthesis of a related phenoxide complex **24** (^{BQ}-NC^OP)Ir^{III}(H)[O(Ph)···HO(Ph)···HOPh] and its partial ¹H NMR spectra at 20 °C. c) ORTEP diagram of **24**. d) Diagrams of the six-membered iridacycle from different directions.

Attempts to isolate **B** have been unsuccessful, making its structural characterization by X-ray diffraction analysis

difficult. One possibility for the low stability of **B** is the facile β -hydride elimination involving the OEt ligand. To our satisfaction, the substitution of PhOH for EtOH led to a stable complex **24**, which was isolated in 92% yield and fully characterized. The isolated **24** exhibits a ^{31}P NMR signal at δ 159.8 ppm in C_6D_6 , which is very similar to that observed for **B** in terms of the chemical shift. The notable ^1H NMR signals includes a doublet at δ -34.28 ($J_{\text{P-H}} = 24.0$ Hz at 20 $^\circ\text{C}$) for Ir-H, and a broad singlet at δ 9.40 ppm corresponding to two OH groups and peaks in the range of 6.66 to 6.99 ppm corresponding to three PhO groups (Figure 2b). The solid-state structure of **24** was revealed by X-ray diffraction analysis, which shows two hydrogen-bonds, one between the OPh ligand and an uncoordinated PhOH ($d_{\text{O1}\cdots\text{H3}} = 1.643$ Å, $d_{\text{O1}\cdots\text{O3}} = 2.469$ Å), and the other between the uncoordinated PhOH and another PhOH that is coordinated to the metal ($d_{\text{O3}\cdots\text{H2}} = 1.875$ Å, $d_{\text{O3}\cdots\text{O2}} = 2.649$ Å). Such multiple interactions introduced by these two PhOH molecules result in the formation of a novel six-membered iridacycle, which is nearly coplanar, as illustrated in Figure 2d. The observation of only one set of signals for the three PhO groups in $(^{BQ}\text{-NC}^{\text{OP}})\text{Ir}^{\text{III}}(\text{H})[\text{O}(\text{Ph})\cdots\text{HO}(\text{Ph})\cdots\text{HOPh}]$ **24** (Figure 2b) indicates that the barrier to the exchange between the coordinated and uncoordinated PhOH molecules is low.

On the basis of NMR data and the structural information for the closely related complexes **24**, it is reasonable to propose that **B** $(^{BQ}\text{-NC}^{\text{OP}})\text{Ir}^{\text{III}}(\text{H})[\text{O}(\text{Et})\cdots\text{HO}(\text{Et})\cdots\text{HOEt}]$ contains a six-membered iridacycle with two hydrogen-bonds involving one EtO ligand and two EtOH molecules. The notable downfield shift of the Ir-H resonance for **B** is consistent with the formation of the six-coordinate Ir(III) species, wherein the coordination site *trans* to the hydride is occupied by one Ir-bound EtOH. The resonances for two EtOH molecules participating in the hydrogen-bond interactions cannot be distinguished from that for the excess, free EtOH molecules present in the solution, even at -75 $^\circ\text{C}$. The results indicate that the EtOH molecules in the six-membered cycle interchange rapidly with the free EtOH molecules on the NMR time scale, presumably through the disruption of the hydrogen-bondings to form the five-coordinate species $(^{BQ}\text{-NC}^{\text{OP}})\text{Ir}^{\text{III}}(\text{H})(\text{OEt})$ **C** (eq 9), which is in accordance with the line-broadening behavior detected by the ^{31}P NMR experiment. Kinetic profiles and kinetic and equilibrium isotope effects, as discussed in the following sections, provide additional support for the structural assignment of **B** and for its interconversion with **C**.



In short, the catalyst resting state depends on the nature of the substrates: the reactions of 1-oct and styrene, and probably of other α -olefins, have **A**_(alkene) as the major resting state throughout the catalytic process, while the reactions of COE, and probably of other multisubstituted alkenes mainly adopt **B** as the resting state. These out-

comes can be rationalized by the lower binding affinity of 1,2-disubstituted alkenes to the Ir(I) center in **[Ir]** relative to monosubstituted alkenes, presumably due to the dominant influence of steric effects.

2.7.2. Kinetics Studies. Next we studied the kinetics for the Ir-catalyzed TH reactions (Figure 3). The adoption of different resting states promoted a comparative examination of the kinetics between mono- and multisubstituted alkenes. Because the isomerization of 1-oct occurs readily under the catalytic conditions, we therefore chose styrene as the substrate, which permits kinetic studies without the complication introduced by the isomerization.

The reaction rates for the catalytic TH of both COE and styrene are first-order in the precatalyst **6** (Figure 3). The dependence of the reactions rates on the substrate concentration, however, varies significantly according to the substrate. Plotting $\log(\text{rate})$ versus $\log[\text{COE}]$ yields a straight line of slope 0.04, implying a zeroth-order dependence on $[\text{COE}]$ (Figure 3a), whereas plotting $\log(\text{rate})$ versus $\log[\text{styrene}]$ yields a straight line of slope -0.92, showing an inverse first-order dependence on $[\text{styrene}]$ (Figure 3b).

Accessing the dependence of reactions rates on $[\text{EtOH}]$ is more complicated. At low $[\text{EtOH}]$ (<1.0 M), we observed the catalyst decomposition during the TH process of COE. Thus, the ethanol concentration was varied between 1.0 and 8.0 M, while keeping the **[6]** and **[COE]** constant at 20.0 mM and 1.0 M respectively. Plotting $\log(\text{rate})$ versus $\log[\text{EtOH}]$ yields a straight line of slope -0.23, showing a negative dependence on $[\text{EtOH}]$ (Figure 3a). For the TH of styrene, the iridium catalyst exhibits good stability even at $[\text{EtOH}]$ as low as 0.4 M. In the low $[\text{EtOH}]$ range (0.4-1.0 M), a positive dependence on $[\text{EtOH}]$ (slope: 0.74) was observed. In the higher concentration range (1.0-3.5 M), the positive dependence on $[\text{EtOH}]$ remained, albeit with a lower order (slope: 0.38), likely caused by the gradual saturation in EtOH (Figure 3b). Thus, under the typical catalytic conditions, the catalysis of COE is inhibited by EtOH, whereas the reaction rate for the catalysis of styrene is enhanced at higher $[\text{EtOH}]$.

2.7.3. Kinetic Isotope Effects. To probe the rate-determining step (RDS), kinetic isotope effects have been studied by comparing the reaction rates using deuterated hydrogen donors. Under the typical catalytic conditions ($[\text{ethanol}]$ (15.6 M) is much greater than $[\text{COE}]$ (0.5 M), and **[6]** is 7.5 mM), measuring the initial rates of the TH reactions of COE (<20% conversion) using EtOH and $\text{C}_2\text{D}_5\text{OD}$ in separate vessels at 26 $^\circ\text{C}$ revealed a primary kinetic isotope effect ($\text{KIE}_{\text{COE1}} = k_{\text{EtOH}}/k_{\text{C}_2\text{D}_5\text{OD}} = 1.98$). Because the observed KIE may arise from the α -C-H/D or O-H/D cleavage, $\text{C}_2\text{D}_5\text{OD}$ was thus replaced with EtOD to determine the origin of the KIE. Remarkably, an *inverse* KIE was consistently obtained for the reactions with EtOH versus EtOD ($\text{KIE}_{\text{COE2}} = k_{\text{EtOH}}/k_{\text{EtOD}} = 0.68$) (Figure 4a).

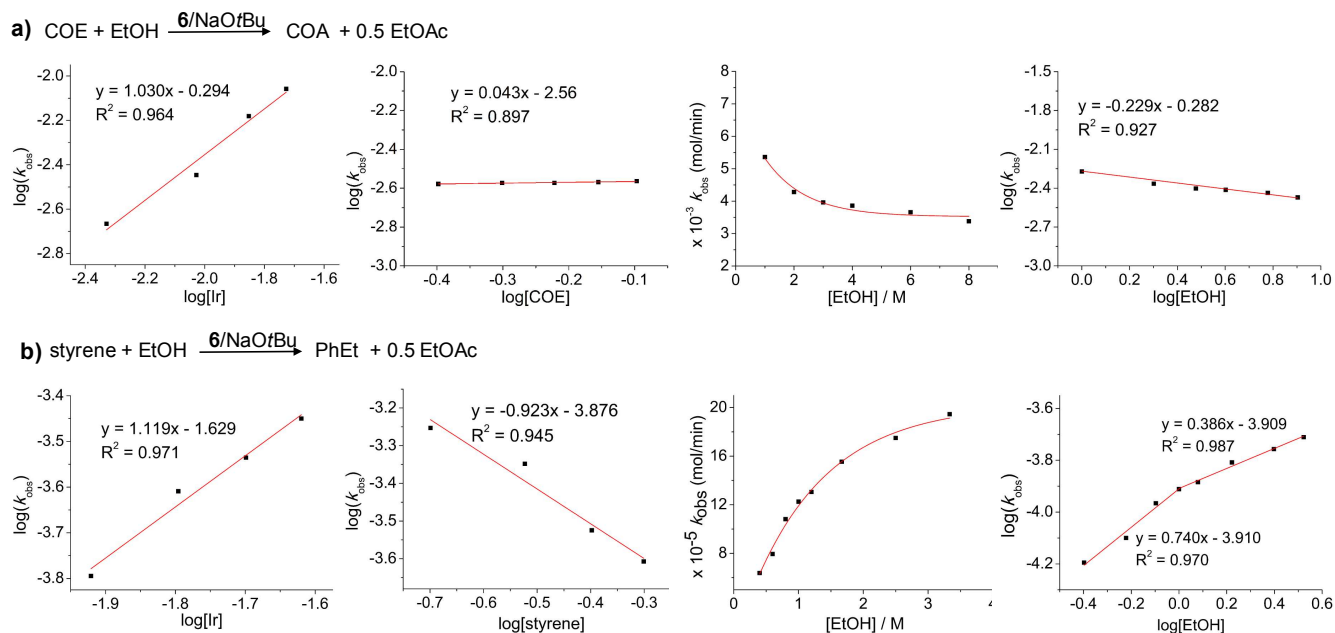


Figure 3. Kinetic profiles for Ir-catalyzed TH reactions of COE (a) and styrene (b) with EtOH.

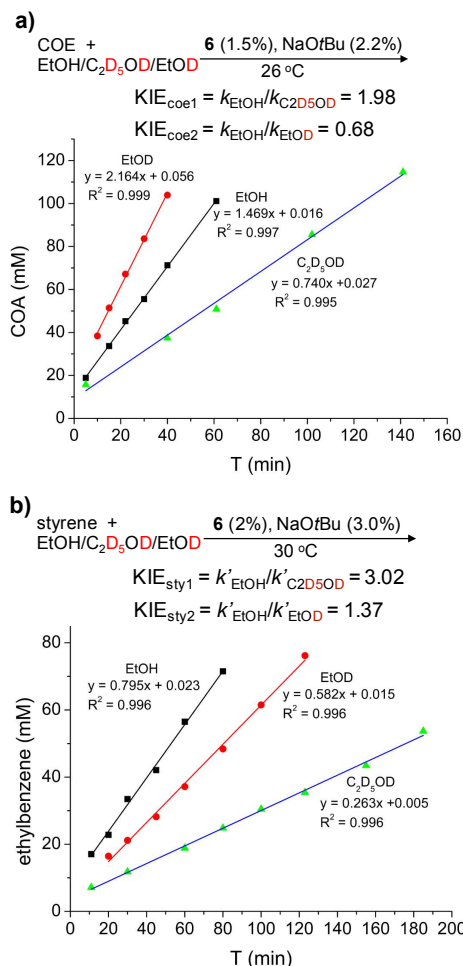


Figure 4. Kinetic isotope effect measurements for a) TH reactions of COE with EtOH, C₂D₅OD, and EtOD, and b) TH reactions of styrene with EtOH, C₂D₅OD, and EtOD.

Comparison of the initial rates for the reactions of styrene (<20% conversion) using EtOH versus C₂D₅OD at 30 °C, again, established a primary KIE ($\text{KIE}_{\text{sty1}} = k'_{\text{EtOH}}/k'_{\text{C}_2\text{D}_5\text{OD}} = 3.02$), which in fact is larger than that observed for COE ($\text{KIE}_{\text{COE1}} = 1.96$). In contrast to the *inverse* KIE obtained in the reactions of COE with EtOH versus EtOD ($\text{KIE}_{\text{COE2}} = 0.68$), the reactions of styrene with EtOH versus EtOD gave a normal KIE, albeit with a small value ($\text{KIE}_{\text{sty2}} = k'_{\text{EtOH}}/k'_{\text{EtOD}} = 1.37$) (Figure 4b).

The primary KIEs observed for both reactions of COE and styrene (KIE_{COE1} and KIE_{sty1}), coupled with the kinetic data presented above, suggest that β -hydride elimination of complex (^{BQ}-NC^{OP})Ir^{III}(H)(OEt) **C** most likely constitutes the RDS, regardless of the alkene substrates.

2.7.4. Equilibrium Isotope Effects. In order to place these differing KIEs (a normal KIE_{sty2} versus an inverse KIE_{COE2}) observed for the reactions with EtOH versus EtOD in context, it is important to understand how the change in the OH* group (H* = H or D) of the hydrogen donor affect the equilibrium isotope effects (EIEs) for the reversible elementary steps prior to the RDS.

The inverse first-order dependence on [styrene] observed in the catalysis of styrene indicates that the decomplexation of alkene from **A**_(sty) (**A**_(sty) → **[Ir]**) and the oxidative addition of EtOH to **[Ir]** (**[Ir]** → **C**) occur reversibly prior to the RDS (Figure 5). Because the catalytic process has the styrene adduct **A**_(sty) as the resting state, the occurrence of the normal KIE_{sty2} (1.37) obtained in the reactions of styrene with EtOH versus EtOD is readily accounted for by a normal $\text{EIE}_{[\text{Ir}] \rightarrow \text{C}}$ for the interconversion of **[Ir]** and **C**, assuming the magnitude of the isotope effect arising from the following β -hydride elimination of (^{BQ}-NC^{OP})Ir^{III}(H*)(OEt) **C** (H*: H versus D) is very small. The pre-equilibrium formation of **C** via the oxidative addition of EtOH* to the Ir(I) center in **[Ir]** is considered to be more favorable for EtOH than EtOD because the zero-

point energy difference between O–H and O–D would be expected to be greater than that between Ir–H and Ir–D, according to the rule that “the heavier atom favors the stronger bond”.³⁴

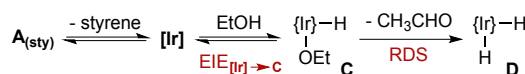
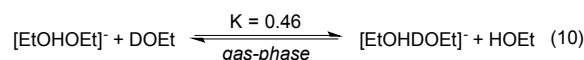


Figure 5. The sequence for the interconversion of $A_{\text{(sty)}}$ and C prior to the RDS.

The inverse KIE_{COE_2} (0.68) observed for the reaction of COE with EtOH versus EtOD is more difficult to be interpreted. Given the factor that the TH of COE has B as the resting state and β -hydride elimination of C is the RDS, the inverse KIE_{COE_2} may reflect an inverse EIE for the interconversion of B and C ($EIE_{B \rightarrow C}$). The pre-equilibrium formation of C ($^{\text{BQ-NC}^{\text{OP}}}\text{Ir}^{\text{III}}(\text{H})(\text{OEt})$) from the resting state B via the release of two H-bound EtOH molecules, is presumably less favorable than the release of the D-bound EtOD molecules. In line with this contention, Dixon and coworkers have previously reported that the H-bound ethoxide dimer is more stable than the D-bound dimer in the gas-phase with an equilibrium constant of ~ 0.46 for eq 10.³⁵



We have been unable to observe C , rendering the direct measurement of $EIE_{B \rightarrow C}$ not feasible. Thus, we sought to measure the equilibrium constant for $B + \text{COE} \leftrightarrow A_{\text{(COE)}} + 3 \text{EtOH}^*$. The interconversion of B and $A_{\text{(COE)}}$ entails the following sequence: (1) dissociation of two EtOH^* molecules ($B \rightarrow C$); (2) reductive elimination of EtOH^* in C ($C \rightarrow [\text{Ir}]$); and (3) alkene complexation to $[\text{Ir}]$ ($[\text{Ir}] \rightarrow A_{\text{(COE)}}$) (cf. Figure 6). In principle, the nature of alkene should have no influence on the $EIE_{B \rightarrow A(\text{alkene})}$. Thus, the observed $EIE_{B \rightarrow A(\text{alkene})}$ is a composite that includes the $EIE_{B \rightarrow C}$ for ethanol dissociation and the $EIE_{C \rightarrow [\text{Ir}]}$ for reductive elimination of ethanol (i.e., $EIE_{B \rightarrow A(\text{alkene})} = EIE_{B \rightarrow C} \times EIE_{C \rightarrow [\text{Ir}]}$).

While B is the only detectable species (vide supra) under the catalytic conditions with $[\text{EtOH}]$ being much greater than $[\text{COE}]$, increasing $[\text{COE}]$ relative to $[\text{EtOH}]$ did permit the observation of both B and $A_{\text{(COE)}}$. Treatment of **6** (20 mM) with NaOtBu (44 mM), COE (1 M), and EtOH^* (2 M) in C_6D_6 at 20 °C in 10 min resulted in a 0.11:1 $A_{\text{(COE)}}:B$ ratio for EtOH and a 0.19:1 $A_{\text{(COE)}}:B$ ratio for EtOD (the conversion of COE to COA was $<5\%$ at this point). The data yield $K = 0.88 \text{ M}^2$ for $B + \text{COE} \leftrightarrow A_{\text{(COE)}} + 3 \text{EtOH}$ and 1.52 M^2 for $B + \text{COE} \leftrightarrow A_{\text{(COE)}} + 3 \text{EtOD}$, corresponding to an inverse $EIE_{B \rightarrow A(\text{COE})}$ of 0.58 (Figure 6).

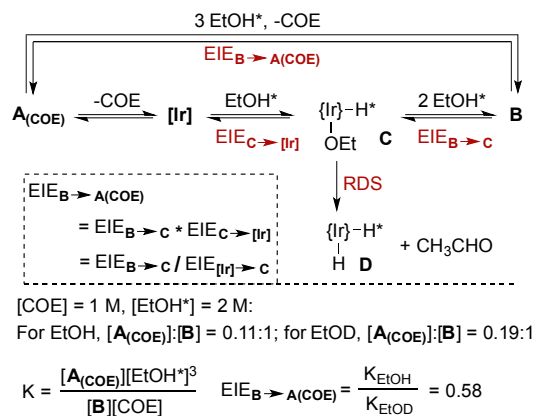


Figure 6. Equilibrium isotope effect measurements for $B + \text{COE} \leftrightarrow A_{\text{(COE)}} + 3 \text{EtOH}$ at 20 °C by NMR spectroscopies.

Applying this value of $EIE_{B \rightarrow A(\text{COE})}$ (0.58) and the value of KIE_{sty_2} (1.37) (though not rigorous, the normal KIE_{sty_2} (1.37), to a certain extent, reflects a normal $EIE_{[\text{Ir}] \rightarrow C}$ for the interconversion of $[\text{Ir}]$ and C , that is, an inverse $EIE_{C \rightarrow [\text{Ir}]}$ for the interconversion of C and $[\text{Ir}]$, according to the aforementioned analysis) to eq 11, we obtain a value of 0.79 for $EIE_{B \rightarrow C}$.

$$EIE_{B \rightarrow C} = EIE_{B \rightarrow A(\text{COE})} \times EIE_{[\text{Ir}] \rightarrow C} \quad (11)$$

$$= EIE_{B \rightarrow A(\text{COE})} \times KIE_{\text{sty}_2} = 0.58 \times 1.37 = 0.79$$

Taking into account of the different reaction parameters (concentration and temperatures), the $EIE_{B \rightarrow C}$ value is comparable to the KIE_{COE_2} value (0.68). These data support the assertion that the inverse KIE_{COE_2} is associated with the pre-equilibrium formation of C from B , via the release of two H-bound ethanol molecules.

2.7.5. Proposed Mechanism. A sizable body of data has been obtained, which indicate that the catalytic processes for the TH of COE and styrene/1-oct with EtOH exhibit fundamentally different characteristics. A mechanism consistent with the experimental observations is depicted Figure 7.

For the reaction of COE, the iridium precatalyst **6** reacts with NaOtBu to form the $14e^-$ species $[\text{Ir}]$, which is further converted to $(^{\text{BQ-NC}^{\text{OP}}}\text{Ir}^{\text{III}}(\text{H})(\text{OEt}))$ **C** via the oxidative addition of EtOH. Complex **C** binds to two EtOH molecules reversibly to give **B**, which has been determined to be the off-cycle resting state. In the RDS, the five-coordinate ethoxy complex **C** undergoes β -hydride elimination to form an Ir(III) dihydride species **D** and release acetaldehyde. The latter then reacts with EtOH to yield hemiacetal, which is subsequently dehydrogenated to give EtOAc. The primary KIE_{COE_1} observed in the reaction of COE with EtOH versus $\text{C}_2\text{D}_5\text{OD}$ supports the proposed RDS. Moreover, the kinetic data of first-order in the catalyst and negative order in EtOH, as well as the inverse KIE_{COE_2} observed in the experiments of EtOH versus EtOD, are in accordance with the proposed catalyst resting state and the RDS.

A key difference between the reactions of COE and styrene/1-oct is the resting state. The thermodynamic stabil-

ity of $A_{\text{(sty)}}$ or $A_{\text{(1-oct)}}$ results in its dominance and inhibition on catalysis, which is consistent with the observed inverse first order dependence on [styrene] and positive dependence on [EtOH]. Regardless of the alkene used, β -hydride elimination constitutes the RDS, as judged by the primary KIE_{sty}.

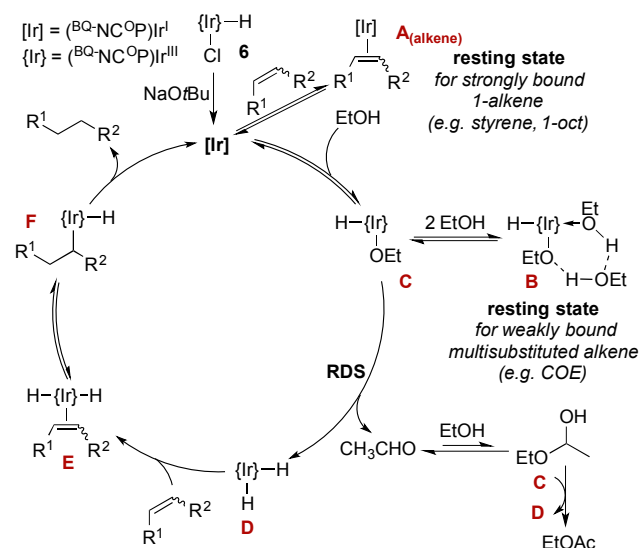
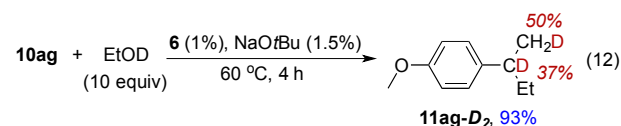


Figure 7. Proposed mechanism.

The rate dependence on the substrate concentration (zeroth order in COE and inverse first order in styrene) is consistent with the conclusion that the coordination of alkene to the dihydride complex **D**, and the following hydride migratory insertion in **E** occur after the RDS. Provided the observation of H/D scrambling in the TH of **23** with C_2D_5OD (see Table 4), we have concluded that the alkene inserting into Ir-H/D bonds is reversible. Reductive elimination of Ir(III) hydrido alkyl complex **F** releases the hydrogenated product and regenerates [Ir].

Although we have not detected the dihydride species **D** directly by NMR spectroscopic methods, the relevant PCP pincer-ligated Ir(III) dihydride complexes have been well-documented.^{18,36} Furthermore, treatment of **10ag** with EtOD (10 equiv) under the catalytic conditions led to **11ag-D₂** with 37% D-content at the tertiary carbon and 50% D-content in the attached Me group (eq 12). Considering that **10ag** undergoes selective 1,2-insertion as concluded from the reaction of **10ag** and C_2D_5OD (see Section 2.6), the incorporation of D-atom to both carbons of the C-C double bond at such levels provides evidence in support of the occurrence of $(^{BQ}NC^OP)Ir(H)(D)$ intermediate.



2.7.6. EtOH versus iPrOH. The information gained in the mechanistic studies indicates that EtOH can be an inhibitor of the catalytically active intermediate **C** due to the formation of the off-cycle resting state **B**. We envisioned that such an inhibition effect might be dimin-

ished/vanished by using *i*PrOH as the hydrogen donor, assuming the hydrogen-bonding interactions between the *i*PrO ligand and *i*PrOH, if present, would be weaker than those in **B**. Consistent with the premise, a comparison of the reaction rates revealed that the TH of COE with *i*PrOH is significantly faster (~20 times) than that with EtOH (Figure 8a).

In sharp contrast, the reaction of styrene with *i*PrOH was found to be ~2 times slower than that with EtOH (Figure 8b). In this case, the high affinity of styrene to the Ir(I) center in [Ir] causes the catalytic inhibition by the substrate, rather than the hydrogen donor, and the dehydrogenation reactivity of the alcohol now exerts influence on the overall catalytic efficiency. The primary alcohol, EtOH, is more reactive towards the dehydrogenation than the secondary alcohol, *i*PrOH, accounting for the superior performance of the former in the TH of styrene.

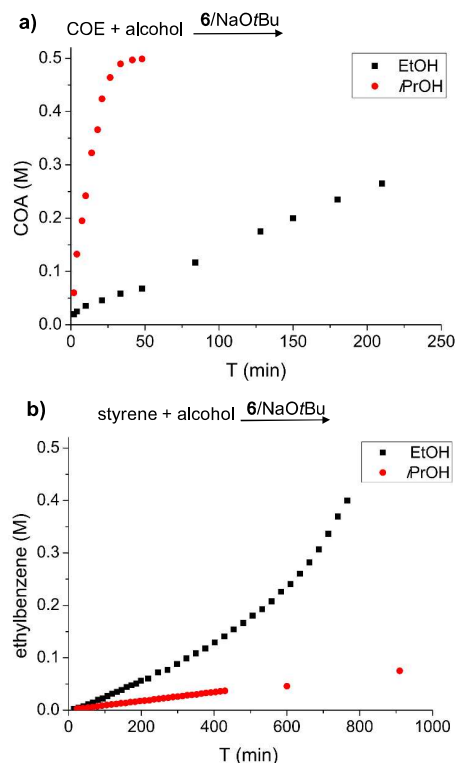


Figure 8. Ir-catalyzed TH of styrene (**a**) and COE (**b**) with EtOH and *i*PrOH.

2.7.7. (NCP)Ir versus (PCP)Ir. One question needs to be answered is why $(^{BQ}NC^OP)Ir$ complex is capable of catalyzing the TH of alkene with EtOH, while the closely related (PCP)Ir and (POCOP)Ir complexes effect neglectable catalysis for the same transformation. To address this issue, the reaction of 1-oct with EtOH catalyzed by the (PCP)Ir complex was probed. Monitoring the reaction in the presence of (PCP)IrHCl (5 mol% relative to 1-oct) and NaOtBu (7.5 mol%) in C_6D_6 by NMR revealed the formation of a mixture of *trans* and *cis* isomers of $(PCP)Ir^{III}(H)(CO)(Me)$ **25** at the early stage of the reaction (~10 min). These carbonyl complexes remained as the dominant species over the course of 12 h, and a minimal

catalytic activity for the TH was observed (<5% conversion of 1-oct to octane).

The *trans* and *cis* mixture was isolated (94% total yield) from an independent experiment conducted in toluene (Figure 9). The characteristic NMR resonances for the major species, *trans*-**25**, include a ^1H NMR triplet at δ -11.07 for Ir-H and a broad singlet at δ 0.10 ppm for Ir-Me, and a ^{13}C NMR triplet at δ -182.3 ppm for Ir-CO. Moreover, the solid-state structure of *trans*-**25** has been determined by X-ray diffraction analysis (Figure 9). On the basis of these data and precedents regarding relevant pincer Ir-mediated decarbonylation of EtOH³⁷ and MeOH,³⁸ a pathway involving the (PCP)Ir-mediated ethanol dehydrogenation, followed by the decarbonylation of the resulting acetaldehyde, seems to be a reasonable one for the formation of **25** (see Supporting Information).

It is important to note that the facile decarbonylation of acetaldehyde leads to inactive Ir(III) carbonyl complexes **25**,^{37,38} which is responsible for the ineffectiveness of the PCP iridium system in the TH with EtOH. In the case of the NCP iridium system, EtOAc is the sole byproduct observed for the TH reaction, indicating that the conversion of acetaldehyde to EtOAc must be significantly faster than the decarbonylation, which partly account for the efficacy of the ($^{\text{BQ}}\text{-NC}^{\text{OP}}$)Ir/EtOH combination for the catalytic TH.

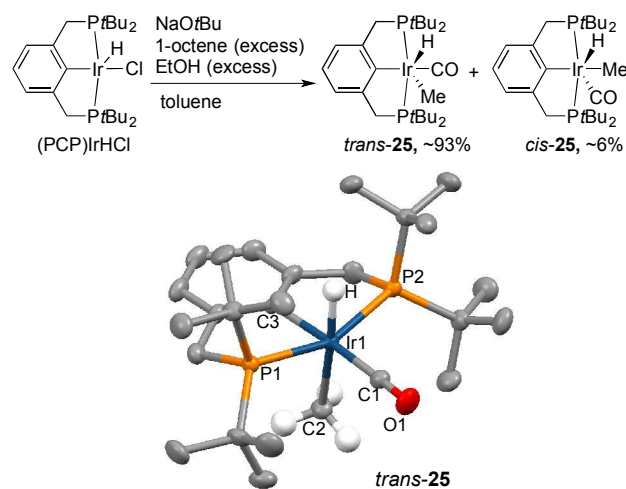


Figure 9. Formation of (PCP)Ir^{III}(H)(CO)(Me) **25** via (PCP)Ir-mediated decarbonylation of EtOH, and ORTEP diagram of *trans*-**25**.

3. CONCLUSIONS

We have demonstrated, for the first time, that low-cost, renewable ethanol can serve as a general reductant for hydrogenation of a wide variety of C-C multiple bonds. The success of this transformation can in part be attributed to the facile conversion of acetaldehyde, the initial EtOH dehydrogenation product, into ethyl acetate, thus eliminating the possibility of catalyst poisoning by the aldehyde. The scope of this TH process is very broad, covering unactivated alkyl alkenes, aryl alkenes, electron-rich/deficient olefins, *O*- and *N*-heteroarenes, and inter-

nal alkynes, some of which would be challenging to be reduced by known transfer hydrogenation means. The tolerance of many functional groups, high chemoselectivity, and formation of low-toxic byproduct (EtOAc), make the ($^{\text{BQ}}\text{-NC}^{\text{OP}}$)Ir/EtOH combination an attractive catalytic system for selective hydrogenation of C-C multiple bonds.

The mechanism of ($^{\text{BQ}}\text{-NC}^{\text{OP}}$)Ir-catalyzed transfer hydrogenation of alkene with EtOH has been elucidated. Some important features include the following:

(1) Decarbonylation of acetaldehyde by ($^{\text{BQ}}\text{-NC}^{\text{OP}}$)Ir appears to be less feasible than that by (PCP)Ir. Such a difference is likely electronic in nature, considering that the $^{\text{BQ}}\text{-NC}^{\text{OP}}$ ligand is less electron-donating than PCP as a result of the *t*Bu₂P-to-N($^{\text{BQ}}$) donor substitution, and therefore the formation of (pincer)Ir^{III}(H)(CO)(Me) bearing a strong π -accepting CO ligand at the Ir(III) center would be thermodynamically less favorable for $^{\text{BQ}}\text{-NC}^{\text{OP}}$ relative to PCP.

(2) Although alcohol dehydrogenation is one of the most readily catalyzed reactions of transition metal complexes, the turnover-limiting segment of the TH cycle reported in this work is the ethanol dehydrogenation. Specifically, β -hydride elimination of the ethoxy Ir(III) hydride complex ($^{\text{BQ}}\text{-NC}^{\text{OP}}$)Ir^{III}(H)(OEt) is the rate-determining step. The activation barriers for the hydrogenation of unactivated alkenes (at least monosubstituted and 1,2-disubstituted alkenes) are relatively low.

(3) The reaction rates for the Ir-catalyzed TH are substrate-dependent. For alkenes with strong binding affinity to the three-coordinate Ir(I) center, the catalysis is subject to substrate inhibition; thus, performing the reaction at low [alkene] in neat EtOH would lead to high efficiency. For alkenes that bind weakly to the Ir(I) center, the reversible bonding of two EtOH molecules to ($^{\text{BQ}}\text{-NC}^{\text{OP}}$)Ir^{III}(H)(OEt) results in catalysis inhibition by the hydrogen donor; consequently increasing [alkene] relative to [EtOH] may afford a productive system.

4. EXPERIMENTAL SECTION

Materials and Methods. All manipulations were carried out using standard Schlenk, high-vacuum and glove-box techniques unless otherwise stated. EtOH was freshly distilled from magnesium under argon. Toluene, diethyl ether and tetrahydrofuran (THF) were freshly distilled from sodium benzophenone ketyl prior to use. NMR spectra were recorded on Agilent 400MHz, Agilent 600 MHz and Varian 400MHz at ambient temperature. The residual peak of deuterated solvent was used as a reference for ^1H and ^{13}C chemical shifts. ^{31}P NMR chemical shifts were referenced to an external 85% H₃PO₄ standard.

Synthesis of Benzo[*h*]quinolin-9-ol hydrobromide (8). 9-Methoxybenzo[*h*]quinolone **7** (1.12 g, 0.54 mmol) and a 40% HBr (60 mL) aqueous solution were added to a 250 mL flask. The reaction was heated at 120 °C for 12 h. Yellow-green solid precipitated when the solution cooled to room temperature. After filtration, the precipitate was washed with water (10 mL), cooled EtOH (10 mL), EtOAc (20 mL) and Et₂O (20 mL), affording the product as yel-

low-green solid (1.26 g, 85%). ¹H NMR (400 MHz, DMSO-*d*₆): δ 10.86 (bs, 2H), 9.15 (dd, *J* = 5.1, 1.1 Hz, 1H), 9.00 (d, *J* = 8.0 Hz, 1H), 8.45 (d, *J* = 1.9 Hz, 1H), 8.12 – 7.98 (m, 3H), 7.83 (d, *J* = 8.8 Hz, 1H), 7.47 (dd, *J* = 8.7, 2.1 Hz, 1H). ¹³C NMR (101 MHz, CD₃OD): δ 158.1, 144.5, 143.9, 138.7, 131.1, 130.2, 128.5, 128.2, 127.2, 123.3, 121.7, 121.6, 107.4. Anal. Calcd for C₁₃H₁₀BrNO: C, 56.55; H, 3.65; N, 5.07. Found: C, 56.52; H, 3.87; N, 5.00.

Synthesis of 9-((di-*tert*-butylphosphanyl)oxy)benzo[*h*]quinoline (9). Under argon atmosphere, a solution of **8** (1.1 g, 4.0 mmol) and NaH (0.4 mg, 10.0 mmol, 60% purity) in 15 mL THF in a 100 mL sealed tube was stirred for 0.5 h at room temperature. Di-*tert*-butylchlorophosphine (0.82 mL, 4.8 mmol) was added to the tube. The tube was sealed with a Teflon plug and then heated at 100 °C for 5 h. After evaporation of the solvent under vacuum, the residue was extracted with Et₂O (30 mL) and filtered through a pad of Celite. Brown solid was obtained after removal of Et₂O under vacuum. The solid was washed with a small amount of cold *n*-pentane (2 mL) giving the product as white solid (1.12 g, 81% yield). ¹H NMR (400 MHz, C₆D₆): δ 9.80 (d, *J* = 2.1 Hz, 1H), 8.86 (dd, *J* = 4.3, 1.7 Hz, 1H), 7.69 (m, 1H), 7.63 (d, *J* = 8.7 Hz, 1H), 7.60 (dd, *J* = 8.0, 1.7 Hz, 1H), 7.52 (d, *J* = 8.8 Hz, 1H), 7.24 (d, *J* = 8.8 Hz, 1H), 6.94 (dd, *J* = 8.0, 4.3 Hz, 1H), 1.22 (d, *J* = 11.7 Hz, 18H). ³¹P NMR (162 MHz, C₆D₆): δ 154.5. ¹³C NMR (101 MHz, C₆D₆): δ 159.3 (d, *J* = 9.7 Hz), 148.4, 146.5, 135.1, 133.8, 129.2, 128.9, 127.2, 126.6, 123.1, 121.6, 120.9 (d, *J* = 9.0 Hz), 112.2 (d, *J* = 13.2 Hz), 35.5 (d, *J* = 26.9 Hz), 27.2 (d, *J* = 15.7 Hz). HRMS (EI), *m/z* Calcd for C₂₀H₂₈NP (M⁺) 339.1752, found: 339.1749.

Synthesis of Iridium Complex (¹⁸⁰NC^{OP})IrHCl **6.** Compound **9** (305 mg, 0.9 mmol), [Ir(COD)Cl]₂ (290 mg, 0.43 mmol) and toluene (25 mL) was added in a 100 mL Kontes flask. The flask was sealed with a Teflon plug and then heated at 120 °C for 12 h under a hydrogen atmosphere. After the solvent was removed under vacuum, the residue was washed with pentane in the glovebox. The solid was dried under vacuum to give 0.49 g (83% yield) product as yellow solid. The product (20 mg) was dissolved in THF (2 mL), and pentane (1.0 mL) was added slowly. The solvents evaporated slowly at ambient temperature in the glovebox. After a few days, yellow crystals of **6** (THF) suitable for X-ray analysis were obtained. ¹H NMR (400 MHz, CDCl₃): δ 9.53 (s, 1H), 8.29 (d, *J* = 7.9 Hz, 1H), 7.84 – 7.66 (m, 2H), 7.49 (d, *J* = 8.8 Hz, 1H), 7.41 (d, *J* = 8.3 Hz, 1H), 7.25 (d, *J* = 8.1 Hz, 1H), 1.43 (d, *J* = 14.7 Hz, 9H), 1.37 (d, *J* = 15.1 Hz, 9H), -40.56 (d, *J* = 21.4 Hz, 1H). ³¹P NMR (162 MHz, CDCl₃): δ 162.25 (d, *J* = 19.1 Hz). ¹³C NMR (101 MHz, CDCl₃): δ 163.74, 156.5, 148.9, 140.15, 137.9, 137.6, 129.3, 128.4, 126.8, 122.0 (d, *J* = 3.1 Hz), 121.7, 121.0, 113.5 (d, *J* = 10.1 Hz), 42.4 (d, *J* = 27.5 Hz), 39.1 (d, *J* = 31.0 Hz), 28.1 (d, *J* = 4.4 Hz), 27.7 (d, *J* = 4.2 Hz). Elemental analysis calcd for C₂₁H₂₆ClIrNOP (567.11): C, 44.48; H, 4.62; N, 2.47. Found: C, 44.12; H, 4.44; N, 2.15.

General Procedure for Transfer Hydrogenation of Alkenes with EtOH. In an argon filled glovebox, catalyst **6** (1.25 μmol, 0.7 mg), NaOtBu (5.0 μmol, 0.5 mg), alkene (0.5 mmol) and EtOH (1.0 mL) were added to a 10 mL

dried Schlenk tube. The tube was sealed with a Teflon plug and moved out of the glovebox. The solution was heated at 60 °C for 2 h. The reaction was quenched by exposing the solution to air and concentrated in vacuum and the residue was purified by chromatography on silica gel.

■ ASSOCIATED CONTENT

Supporting Information

The Supporting Information is available free of charge on the ACS Publications web site at DOI:

Crystallographic data for **6**-(THF) (CCDC 1815133), **24** (CCDC 1819101) and *trans*-**25** (CCDC 1819102) are available free of charge via the Internet at <http://pubs.acs.org>.

■ AUTHOR INFORMATION

Corresponding Author

*huangzh@sioc.ac.cn.

Notes

The authors declare no competing financial interest.

■ ACKNOWLEDGMENT

The authors gratefully acknowledge support from National Key R&D Program of China (2016YFA0202900, 2015CB856600), National Natural Science Foundation of China (21432011, 21422209), Chinese Academy of Sciences (XDB20000000, QYZDB-SSW-SLH016), and Science and Technology Commission of Shanghai Municipality (17JC1401200).

■ REFERENCES

- (1) Andersson, P. G.; Munslow, I. J., Eds. *Modern Reduction Methods*; Wiley-VCH Verlag GmbH & Co. KGaA: Weinheim, 2008.
- (2) For selected reviews on transfer hydrogenation reactions, see: (a) Gladiali, S.; Alberico, E. *Chem. Soc. Rev.* **2006**, *35*, 226. (b) Samec, J. S. M.; Backvall, J.-E.; Andersson, P. G.; Brandt, P. *Chem. Soc. Rev.* **2006**, *35*, 237. (c) Ikariya, T.; Blacker, A. J. *Acc. Chem. Res.* **2007**, *40*, 1300. (d) Wang, C.; Wu, X.; Xiao, J. *Chem. Asian. J.* **2008**, *3*, 1750. (e) Dobereiner, G. E.; Crabtree, R. H. *Chem. Rev.* **2010**, *110*, 681. (f) Gunanathan, C.; Milstein, D. *Chem. Rev.* **2014**, *114*, 12024. (g) Wang, D.; Astruc, D. *Chem. Rev.* **2015**, *115*, 6621. (h) Werkmeister, S.; Neumann, J.; Junge, K.; Beller, M. *Chem. Eur. J.* **2015**, *21*, 12226.
- (3) (a) Mellmann, D.; Sponholz, P.; Junge, H.; Beller, M. *Chem. Soc. Rev.* **2016**, *45*, 3954. (b) Bonitatibus, P. J.; Chakraborty, S.; Doherty, M. D.; Siclován, O.; Jones, W. D.; Soloveichik, G. L., *Proc. Natl. Acad. Sci. U.S.A.* **2015**, *112*, 1687. (c) Chakraborty, S.; Piszal, P. E.; Brennessel, W. W.; Jones, W. D. *Organometallics* **2015**, *34*, 5203.
- (4) (a) Schwizer, F.; Okamoto, Y.; Heinisch, T.; Gu, Y.; Pellizzoni, M. M.; Lebrun, V.; Reuter, R.; Köhler, V.; Lewis, J. C.; Ward, T. R. *Chem. Rev.* **2018**, *118*, 142. (b) Bose, S.; Ngo, A. H.; Do, L. H. *J. Am. Chem. Soc.* **2017**, *139*, 8792.
- (5) For selected references on TH of ketones, see: (a) Morris, R. H. *J. Am. Chem. Soc.* **2012**, *134*, 5893. (b) Zuo, W.; Lough, A. J.; Li, Y. F.; Morris, R. H. *Science* **2013**, *342*, 1080. (c) Lagaditis, P. O.; Sues, P. E.; Sonnenberg, J. F.; Wan, K. Y.; Lough, A. J.; Morris, R. H. *J. Am. Chem. Soc.* **2014**, *136*, 1367. (d) Bigler, R.; Huber, R.; Mezzetti, A. *Angew. Chem. Int. Ed.* **2015**, *54*, 5171. (e) Perez, M.; Elangovan, S.; Spannenberg, A.; Junge, K.; Beller, M. *ChemSus-*

Chem **2017**, *10*, 83. (f) Touge, T.; Nara, H.; Fujiwhara, M.; Kayaki, Y.; Ikariya, T. *J. Am. Chem. Soc.* **2016**, *138*, 10084.

(6) For selected references on TH of imines, see: (a) Uematsu, N.; Fujii, A.; Hashiguchi, S.; Ikariya, T.; Noyori, R. *J. Am. Chem. Soc.* **1996**, *118*, 4916. (b) Zhang, G.; Hanson, S. K. *Chem. Commun.* **2013**, 49, 10151. (c) Li, S.; Li, G.; Meng, W.; Du, H. *J. Am. Chem. Soc.* **2016**, *138*, 12956. (d) Shao, Z.; Fu, S.; Wei, M.; Zhou, S.; Liu, Q. *Angew. Chem. Int. Ed.* **2016**, *55*, 14653.

(7) For selected references on TH of polarized alkenes, see: (a) Keinan, E.; Greenspoon, N. *J. Am. Chem. Soc.* **1986**, *108*, 7314. (b) Moritani, Y.; Appella, D. H.; Jurkauskas, V.; Buchwald, S. L. *J. Am. Chem. Soc.* **2000**, *122*, 6797. (c) Lipshutz, B. H.; Servosko, J. M. *Angew. Chem. Int. Ed.* **2003**, *42*, 4789. (d) Otsuka, H.; Shirakawa, E.; Hayashi, T. *Chem. Commun.* **2007**, 1819. (e) Shang, J.-Y.; Li, F.; Bai, X.-F.; Jiang, J.-X.; Yang, K.-F.; Lai, G.-Q.; Xu, L.-W. *Eur. J. Org. Chem.* **2012**, 2012, 02809. (f) Kosal, A. D.; Ashfeld, B. L. *Org. Lett.* **2010**, *12*, 44. (g) Mebi, C. A.; Nair, R. P.; Frost, B. J. *Organometallics* **2007**, *26*, 429. (h) Ding, B.; Zhang, Z.; Liu, Y.; Sugiyama, M.; Imamoto, T.; Zhang, W. *Org. Lett.* **2013**, *15*, 3690.

(8) For selected references on TH of other unsaturated compounds, see: (a) Adam, R.; Cabrero-Antonino, J. R.; Spannenberg, A.; Junge, K.; Jackstell, R.; Beller, M. *Angew. Chem. Int. Ed.* **2017**, *56*, 3216. (b) Wang, C.; Li, C.; Wu, X.; Pettman, A.; Xiao, J. *Angew. Chem. Int. Ed.* **2009**, *48*, 6524. (c) Wu, J.; Wang, C.; Tang, W.; Pettman, A.; Xiao, J. *Chem. Eur. J.* **2012**, *18*, 9525. (d) Talwar, D.; Li, H. Y.; Durham, E.; Xiao, J. *Chem. Eur. J.* **2015**, *21*, 5370. (e) Mai, V. H.; Nikonov, G. I. *Organometallics* **2016**, *35*, 943. (f) Soltani, O.; Ariger, M. A.; Carreira, E. M. *Org. Lett.* **2009**, *11*, 4196.

(9) (a) Jaska, C. A.; Mannes, I. *J. Am. Chem. Soc.* **2004**, *126*, 2698. (b) Dong, H.; Berke, H. *J. Organomet. Chem.* **2011**, *696*, 1803.

(10) (a) Cummings, S. P.; Le, T.-N.; Fernandez, G. E.; Quiambao, L. G.; Stokes, B. J. *J. Am. Chem. Soc.* **2016**, *138*, 6107. (b) Ojha, D. P.; Gadde, K.; Prabhu, K. R. *Org. Lett.* **2016**, *18*, 5062.

(11) (a) Broggi, J.; Jurčík, V.; Songis, O.; Poater, A.; Cavallo, L.; Slawin, A. M. Z.; Cazin, C. S. J. *J. Am. Chem. Soc.* **2013**, *135*, 4588. (b) Hauwert, P.; Maestri, G.; Sprengers, J. W.; Catellani, M.; Elsevier, C. J. *Angew. Chem. Int. Ed.* **2008**, *47*, 3223. (c) Hauwert, P.; Boerleider, R.; Warsink, S.; Weigand, J. J.; Elsevier, C. J. *J. Am. Chem. Soc.* **2010**, *132*, 16900. (d) Drost, R. M.; Bouwens, T.; van Leest, N. P.; de Bruin, B.; Elsevier, C. J. *ACS Catal.* **2014**, *4*, 1349. (e) Wagh, Y. S.; Asao, N. *J. Org. Chem.* **2015**, *80*, 847. (f) Shen, R.; Chen, T.; Zhao, Y.; Qiu, R.; Zhou, Y.; Yin, S.; Wang, X.; Goto, M.; Han, L.-B. *J. Am. Chem. Soc.* **2011**, *133*, 17037. (g) Wienhofer, G.; Westerhaus, F. A.; Jagadeesh, R. V.; Junge, K.; Junge, H.; Beller, M. *Chem. Commun.* **2012**, 48, 4827.

(12) For heterogeneous catalytic transfer hydrogenation of alkenes using iPrOH as the hydrogen donor, see: (a) Alonso, F.; Riente, P.; Yus, M. *Tetrahedron* **2009**, *65*, 10637. (b) Ito, Y.; Ohta, H.; Yamada, Y. M. A.; Enoki, T.; Uozumi, Y. *Chem. Commun.* **2014**, 50, 12123. (c) Imamura, K.; Okubo, Y.; Ito, T.; Tanaka, A.; Hashimoto, K.; Kominami, H. *RSC Adv.* **2014**, *4*, 19883. (d) Long, J.; Zhou, Y.; Li, Y. *Chem. Commun.* **2015**, 51, 2331.

(13) For homogeneous catalytic transfer hydrogenation of alkenes using iPrOH as the hydrogen donor, see: (a) Horn, S.; Albrecht, M. *Chem. Commun.* **2011**, 47, 8802. (b) Zhang, G.; Yin, Z.; Tan, J. *RSC Adv.* **2016**, *6*, 22419. (c) Mai, V. H.; Nikonov, G. I. *Organometallics* **2016**, *35*, 943. (d) Gnanamgari, D.; Moores, A.; Rajaseelan, E.; Crabtree, R. H. *Organometallics* **2007**, *26*, 1226. (e) Sluijter, S. N.; Elsevier, C. J. *Organometallics* **2014**, *33*, 6389. (f) Bolje, A.; Hohloch, S.; Kosmrlj, J.; Sarkar, B. *Dalton Trans.* **2016**, 45, 15983. (g) Mazloomi, Z.; Pretorius, R.; Pàmies, O.; Albrecht, M.; Diéguez, M. *Inorg. Chem.* **2017**, *56*, 11282.

(14) Zweifel, T.; Naubron, J.-V.; Büttner, T.; Ott, T.; Grützmacher, H. *Angew. Chem. Int. Ed.* **2008**, *47*, 3245.

(15) Siva Reddy, A.; Kumara Swamy, K. C. *Angew. Chem. Int. Ed.* **2017**, *56*, 6984.

(16) (a) Castellanos-Blanco, N.; Flores-Alamo, M.; García, J. *J. Organometallics* **2012**, *31*, 680. (b) Tsuchiya, Y.; Hamashima, Y.; Sodeoka, M. *Org. Lett.* **2006**, *8*, 4851. (c) Monguchi, D.; Beemelmans, C.; Hashizume, D.; Hamashima, Y.; Sodeoka, M. *J. Organomet. Chem.* **2008**, *693*, 867.

(17) (a) Crabtree, R. H.; Pearman, A. J. *J. Organomet. Chem.* **1978**, *157*, 335. (b) Abu-Hasanayn, F.; Goldman, M. E.; Goldman, A. S. *J. Am. Chem. Soc.* **1992**, *114*, 2520. (c) Beck, C. M.; Rathmill, S. E.; Park, Y. J.; Chen, J.; Crabtree, R. H.; Liable-Sands, L. M.; Rheingold, A. L. *Organometallics* **1999**, *18*, 5311. (d) Klei, S. R.; Golden, J. T.; Tilley, T. D.; Bergman, R. G. *J. Am. Chem. Soc.* **2002**, *124*, 2092. (e) Yung, C. M.; Skaddan, M. B.; Bergman, R. G. *J. Am. Chem. Soc.* **2004**, *126*, 13033. (f) Zhang, J.; Gandelman, M.; Shimon, L. J. W.; Rozenberg, H.; Milstein, D. *Organometallics* **2004**, *23*, 4026. (g) Hasegawa, M.; Segawa, Y.; Yamashita, M.; Nozaki, K. *Angew. Chem. Int. Ed.* **2012**, *51*, 6956.

(18) (a) Gupta, M.; Hagen, C.; Kaska, W. C.; Cramer, R. E.; Jensen, C. M. *J. Am. Chem. Soc.* **1997**, *119*, 840.

(19) Göttker-Schnetmann, I.; White, P.; Brookhart, M. *J. Am. Chem. Soc.* **2004**, *126*, 1804.

(20) For selected reviews on transfer dehydrogenation reactions, see: (a) Choi, J.; MacArthur, A. H. R.; Brookhart, M.; Goldman, A. S. *Chem. Rev.* **2011**, *111*, 1761. (b) Gunanathan, C.; Milstein, D. *Science* **2013**, *341*, 1229712. (c) Kumar, A.; Bhatti, T. M.; Goldman, A. S. *Chem. Rev.* **2017**, *117*, 12357. (d) Tang, X.; Jia, X.; Huang, Z. *Chem. Sci.* **2018**, *9*, 288. For selected works on transfer dehydrogenation reactions, see: (e) Xu, W.; P. Rosini, G.; Krogh-Jespersen, K.; Goldman, A. S.; Gupta, M.; Jensen, C. M.; Kaska, W. C. *Chem. Commun.* **1997**, 2273. (f) Liu, F.; Pak, E. B.; Singh, B.; Jensen, C. M.; Goldman, A. S. *J. Am. Chem. Soc.* **1999**, *121*, 4086. (g) Renkema, K. B.; Kissin, Y. V.; Goldman, A. S. *J. Am. Chem. Soc.* **2003**, *125*, 7770. (h) Göttker-Schnetmann, I.; Brookhart, M. *J. Am. Chem. Soc.* **2004**, *126*, 9330. (i) Goldman, A. S.; Roy, A. H.; Huang, Z.; Ahuja, R.; Schinski, W.; Brookhart, M. *Science* **2006**, *312*, 257. (j) Huang, Z.; Brookhart, M.; Goldman, A. S.; Kundu, S.; Ray, A.; Scott, S. L.; Vicente, B. C. *Adv. Synth. Catal.* **2009**, *351*, 188. (k) Kundu, S.; Choliy, Y.; Zhuo, G.; Ahuja, R.; Emge, T. J.; Warmuth, R.; Brookhart, M.; Krogh-Jespersen, K.; Goldman, A. S. *Organometallics* **2009**, *28*, 5432. (l) Yao, W.; Zhang, Y.; Jia, X.; Huang, Z. *Angew. Chem. Int. Ed.* **2014**, *53*, 1390. (m) Bézier, D.; Brookhart, M. *ACS Catalysis* **2014**, *4*, 3411. (n) Zhang, Y.; Fang, H.; Yao, W.; Leng, X.; Huang, Z. *Organometallics* **2016**, *35*, 181. (o) Jia, X.; Huang, Z. *Nat. Chem.* **2016**, *8*, 157. (p) Press, L. P.; Kosanovich, A. J.; McCulloch, B. J.; Ozerov, O. V. *J. Am. Chem. Soc.* **2016**, *138*, 9487. (q) Shih, W.-C.; Ozerov, O. V. *Organometallics* **2017**, *36*, 228.

(21) (a) Jia, X.; Zhang, L.; Qin, C.; Leng, X.; Huang, Z. *Chem. Commun.* **2014**, 50, 11056. (b) Wang, Y.; Qin, C.; Jia, X.; Leng, X.; Huang, Z. *Angew. Chem. Int. Ed.* **2017**, *56*, 1614. (c) Guo, L.; Ma, X.; Fang, H.; Jia, X.; Huang, Z. *Angew. Chem. Int. Ed.* **2015**, *54*, 4023. (d) Yao, W.; Ma, X.; Guo, L.; Jia, X.; Hu, A.; Huang, Z. *Tetrahedron Lett.* **2016**, *57*, 2919. (e) Jia, X.; Huang, Z. *Sci. China: Chem.* **2015**, *58*, 1340.

(22) For selected references for the catalytic conversion of primary alcohols to esters, see (a) Gunanathan, C.; Milstein, D. *Acc. Chem. Res.* **2011**, *44*, 588. (b) Zhang, J.; Leitun, G.; Ben-David, Y.; Milstein, D. *J. Am. Chem. Soc.* **2005**, *127*, 10840. (c) Gunanathan, C.; Ben-David, Y.; Milstein, D. *Science* **2007**, *317*, 790. (d) Chakraborty, S.; Lagaditis, P. O.; Förster, M.; Bielinski, E. A.; Hazari, N.; Holthausen, M. C.; Jones, W. D.; Schneider, S. *ACS Catalysis* **2014**, *4*, 3994. (e) Espinosa-Jalapa, N. A.; Kumar, A.; Leitun, G.; Diskin-Posner, Y.; Milstein, D. *J. Am. Chem. Soc.* **2017**, *139*, 11722.

(23) Wang, Y.; Li, Y.; Huang, Z. unpublished results.

- (24) Aramoto, H.; Obora, Y.; Ishii, Y. *J. Org. Chem.* **2009**, *74*, 628.
- (25) Using 5 μmol complex **6** and 5 μmol NaOtBu.
- (26) von Schenck, H.; Strömberg, S.; Zetterberg, K.; Ludwig, M.; Åkermark, B.; Svensson, M. *Organometallics* **2001**, *20*, 2813.
- (27) Wang, X.; Rinaldi, R. *Energy Environ. Sci.* **2012**, *5*, 8244.
- (28) Campos, J.; Hintermair, U.; Brewster, T. P.; Takase, M. K.; Crabtree, R. H. *ACS Catalysis* **2014**, *4*, 973.
- (29) (a) Grotjahn, D. B.; Larsen, C. R.; Gustafson, J. L.; Nair, R.; Sharma, A. *J. Am. Chem. Soc.* **2007**, *129*, 9592. (b) Vasseur, A.; Bruffaerts, J.; Marek, I. *Nat. Chem.* **2016**, *8*, 209.
- (30) Elderfield, R. C.; Losin, E. T. *The J. Org. Chem.* **1961**, *26*, 1703.
- (31) Louie, J.; Bielawski, C. W.; Grubbs, R. H. *J. Am. Chem. Soc.* **2001**, *123*, 11312.
- (32) Kanzelberger, M.; Singh, B.; Czerw, M.; Krogh-Jespersen, K.; Goldman, A. S. *J. Am. Chem. Soc.* **2000**, *122*, 11017.
- (33) Complex **B** could be synthesized in situ independently by the reaction of **6** with NaOtBu in the presence of 170 equiv of EtOH in C_6D_6 , but it was detectable only at the early stages of the reaction (~ 5 min) at RT. After 5 min, **B** decayed to unidentified species. **B** was reasonably stable during the catalytic TH process of COE with EtOH, but decayed upon the completion of the COE reduction.
- (34) (a) Laidler K. J. *Chemical Kinetics*, 3rd ed., Harper & Row 1987, p 428-433. (b) Gómez-Gallego, M.; Sierra, M. A. *Chem. Rev.* **2011**, *111*, 4857. 9. (c) Jones, W. D. *Acc. Chem. Res.* **2003**, *36*, 140.
- (35) Ellenberger, M. R.; Farneth, W. E.; Dixon, D. A. *J. Phys. Chem.*, 1981, 85, 4.
- (36) (a) Gupta, M.; Hagen, C.; Flesher, R. J.; Kaska, W. C.; Jensen, C. M. *Chem. Commun.* **1996**, 2083. (b) Göttker-Schnetmann, I.; White, P. S.; Brookhart, M. *Organometallics* **2004**, *23*, 1766. (c) Liu, F.; Goldman, A. S. *Chem. Commun.* **1999**, 655. (d) Punji, B.; Emge, T. J.; Goldman, A. S. *Organometallics* **2010**, *29*, 2702.
- (37) Melnick, J. G.; Radosevich, A. T.; Villagran, D.; Nocera, D. G. *Chem. Commun.* **2010**, 46, 79.
- (38) (a) Kloek, S. M.; Heinekey, D. M.; Goldberg, K. I. *Organometallics* **2006**, *25*, 3007. (b) Morales-Morales, D.; Lee, D. W.; Wang, Z.; Jensen, C. M. *Organometallics* **2001**, *20*, 1144.

Insert Table of Contents artwork here

